LUIVITON: Learned Universal Interoperable VIrtual Try-ON

Cong Cao¹ Xianhang Cheng¹ Jingyuan Liu^{2,1} Yujian Zheng¹ Zhenhui Lin¹ Meriem Chkir¹ Hao Li^{1,3}

¹MBZUAI ²The University of Tokyo ³Pinscreen

{cong.cao, xianhang.cheng, yujian.zheng, zhenhui.lin, meriem.chkir}@mbzuai.ac.ae jliucb@connect.ust.hk hao@hao-li.com



Figure 1. LUIVITON, a fully automated and robust virtual try-on system for dressing any humanoid 3D character with arbitrary types of rest-posed 3D clothing models. Given a humanoid 3D model and a clothing item (jacket, suits, pants, dress, etc.), our system automatically determines where the clothing should be placed on the body and how it should be fitted, even for unseen clothing and body, making our system suitable for virtual try-on applications. This figure shows fitting results for a wide variety of clothing onto 3D characters with complex body poses and shapes.

Abstract

We present LUIVITON, an end-to-end system for fully automated virtual try-on, capable of draping complex, multi-layer clothing onto diverse and arbitrarily posed humanoid characters. To address the challenge of aligning complex garments with arbitrary and highly diverse body shapes, we use SMPL as a proxy representation and separate the clothing-to-body draping problem into two correspondence tasks: 1) clothing-to-SMPL and 2) body-to-SMPL correspondence, where each has its unique challenges. While we address the clothing-to-SMPL fitting problem using a geometric learning-based approach for partial-to-complete shape correspondence prediction, we introduce

a diffusion model-based approach for body-to-SMPL correspondence using multi-view consistent appearance features and a pre-trained 2D foundation model. Our method can handle complex geometries, non-manifold meshes, and generalizes effectively to a wide range of humanoid characters—including humans, robots, cartoon subjects, creatures, and aliens, while maintaining computational efficiency for practical adoption. In addition to offering a fully automatic fitting solution, LUIVITON supports fast customization of clothing size, allowing users to adjust clothing sizes and material properties after they have been draped. We show that our system can produce high-quality 3D clothing fittings without any human labor, even when 2D clothing sewing patterns are not available.

1. Introduction

Avatars in games, films, social media, and AR/VR applications span a wide range of realistic, stylized, or fantastical styles, but clothing remains essential for identity and visual coherence. However, modeling and simulating garments are labor-intensive, especially for complex designs. Even when a garment model exists, fitting it to characters with different shapes, poses, or styles remains difficult to automate. Existing solutions rely on procedural fitting of pre-skinned assets, offering limited flexibility for entirely new garments.

Current state-of-the-art methods for virtual try-on face significant limitations. Manual tools like Marvelous Designer [22] or Maya [4] require extensive effort to prepare and simulate garments. While recent learning-based methods [17, 31, 43, 52] automate draping for simple garments, they are restricted by SMPL-only inputs and struggle with multilayer clothing, non-manifold meshes, or stylized characters. They also offer limited control over garment size and personalized customization.

We introduce LUIVITON, a universal virtual try-on framework that automatically drapes arbitrary 3D garments onto a wide range of realistic or stylized humanoid characters while preserving geometric detail and supporting fast garment resizing, as shown in Fig. 1. Unlike prior methods restricted to parametric bodies and manifold clothing, LUIVITON robustly handles diverse body shapes, poses, and complex garment structures, including non-manifold and multilayer designs.

A key challenge lies in establishing reliable clothing-to-body correspondence under large pose variations and partial coverage. Existing methods often fall short in handling such complexity in a generalizable way. To address this, we use SMPL [35] as a proxy representation, and split the problem of directly draping clothing onto the body into two correspondence tasks: 1) between clothing and an SMPL model, and 2) between the input body and an SMPL model, where each has its own unique challenges.

We first predict dense clothing-SMPL correspondences using a geometric learning-based approach. We adopt a deep neural network based on learned diffusion trained on 300 annotated clothing of unique designs. Then the body-SMPL correspondence problem is addressed using appearance features by leveraging pre-trained features obtained from a diffusion model in order to generalize across body types and styles. In particular, we integrate multi-view consistent diffusion features for improved spatial coherence, with highly semantic priors from DINOv2 [40]. A dedicated registration process is then performed between the SMPL model and the input body and clothing using regularized deformation models to suppress correspondence out-

liers and unwanted clothing-body interpenetrations. The clothing is then transferred to the input body shape via simulator-driven deformation in SMPL space, preserving fine topology. Pre-computed correspondences further facilitate fast garment resizing for further adjustments. Our contributions include:

- A universal virtual try-on framework that fully automates garment draping onto arbitrary non-parametric humanoid bodies (realistic or stylized) while handling complex geometries and multilayer stitching.
- A partial-to-complete correspondence prediction model trained on a comprehensive dataset (300 garments with SMPL annotations) to align clothing with SMPL, ensuring robustness to non-manifold meshes and topological variations.
- A body registration technique combining multi-view consistent diffusion features and semantic DINOv2 priors, ensuring generalization across diverse body shapes and poses.
- Fast customization enabling responsive clothing resizing (15 seconds per adjustment) with precomputed correspondences and registrations, streamlining artist workflows.

2. Related Work

Shape Correspondence. Shape correspondence is a fundamental challenge in computer graphics, tackled through geometric matching [10, 14–16, 28, 29], spectral methods [2, 26], and functional mapping [12, 18, 21, 33, 37, 41, 45]. Most approaches focus on category-specific correspondence, struggling with arbitrarily dissimilar objects and non-isometric deformations.

Another way[53] is to learn to extract 2D features from depth images then unproject to 3D. With vision foundation models, 2D semantic features have been improved [1, 20], enhancing robustness across diverse shapes. Our method follows this paradigm by incorporating synchronized multiview diffusion features, further enhancing spatial smoothness and completeness of correspondence.

SMPL Registration. SMPL [35] is a widely used parametric human body model defined by shape and pose parameters. SMPL registration estimates these parameters to align the model with input 3D data.

Early methods relied on pose initialization and texture cues [11], while local approaches improved flexibility but lacked global consistency [56]. Recent learning-based methods like IP-Net [11] predict SMPL parameters directly but struggle with out-of-distribution inputs. The state-of-the-art NICP [38] performs well on human scans but fails on stylized humanoids due to its dependence on geometry alone. Our method addresses this limitation by incorporat-

ing semantic features from vision foundation models to improve robustness across diverse body shapes.

Clothing Draping. Draping garments that are originally not on any human body to a static one is a critical step in simulation pipelines for virtual try-on and digital garment design. Early approaches [32] used rigid alignment based on geometric features but struggled with large pose discrepancies. Later approaches introduced garment skeletons [30], body-part segmentation [44], or mesh partitioning [3, 51] to enable non-rigid deformation, though they often required manual input or were sensitive to segmentation errors. Some methods instead adjust the body to match the garment [25, 54].

More advanced works [17] and [31] can drape various clothing onto different body shapes realistically; however, they require the clothing to be initially draped on a canonical SMPL and only support manifold meshes, limiting their applicability to more complex scenarios.

Cloth Simulation. Cloth simulation is a longstanding challenge in computer graphics. Research is divided into physics-based simulation (PBS) and learning-based methods. PBS models garment dynamics using physical laws [22, 39], achieving high realism but at a high computational cost. Learning-based methods [7–9, 36, 42, 43, 47–49] aim to improve efficiency by predicting garment deformations from human pose and shape. In particular, graph neural networks [23] demonstrate strong generalization ability. For example, ContourCraft [24], the current state-of-the-art method for delicate clothing simulation, has demonstrated strong generalization across various garments and is therefore incorporated into our framework.

3. Method

Fig. 2 provides an overview of our LUIVITON framework, which comprises three main stages. First, we predict dense correspondences detailed in Sec. 3.1 and Sec. 3.2. Second, we perform registration to align SMPL/SMPL+D to clothing and body, described in Sec. 3.3. Finally, the clothing fitting module, outlined in Sec. 3.4, simulates the garment onto the shape of the input character through SMPL shape and pose interpolation.

3.1. Clothing-SMPL Correspondence

To fit an SMPL body into a given 3D garment, it is essential to first establish consistent dense correspondences between the garment and the SMPL model. While state-of-the-art shape correspondence approaches [20] offer a promising direction, directly applying them is non-trivial. The intrinsic partial-to-complete nature of the garment-to-body relationship remains underexplored. Moreover, although gar-

ments and the human body share related semantics, this alone is insufficient for accurate correspondence prediction—semantic ambiguity, such as indistinguishable front and back regions, often leads to errors when relying solely on 2D vision priors [40, 46]. To address these challenges, we adopt a learning-based correspondence network, DiffusionNet [50], which has been shown to be highly effective in partial-to-complete correspondence predictions in connection with functional map approaches. In particular, we are building a dedicated dataset with annotated garments of unique designs for supervised learning.

Dataset Construction. We collect 300 3D garments and annotate vertex-level correspondences between each garment and the SMPL body. Given a 3D garment model with arbitrary topology, we first hire artists to manually drape the garment onto a SMPL body template using Marvelous Designer [22]. We then compute the nearest point on the SMPL body surface for each vertex of the draped garment mesh. Instead of constructing direct 3D-to-3D correspondences, we represent the SMPL body surface as a 2D manifold and define 3D-to-2D correspondences by mapping garment vertices to locations on the SMPL UV map [55], which simplifies the problem significantly.

Our dataset covers a wide range of everyday clothing types, including shirts/T-shirts, sweatshirts, jackets, vests, dresses, jumpsuits, overalls/dungarees, trousers, shorts, skirts, and more. Examples are provided in the Suppl. A.1 in supplementary material.

With access to annotated correspondences, we learn a mapping $g:\mathbb{R}^3\to\mathbb{R}^2$ from the 3D garment to the SMPL UV space in a supervised manner. As shown in Fig. 3, we employ DiffusionNet [50], a lightweight yet powerful architecture for learning on surfaces, to predict this mapping. The mapped 2D UV coordinates on the SMPL body are treated as surface features of the input garment. The network consists of repeated identical blocks that perform feature diffusion over a learned time scale, extract spatial gradients, and apply a shared pointwise MLP at each vertex of the garment mesh. The training loss is defined as:

$$\mathcal{L}_{dif} = \sum_{i=1}^{N} ||x_i - g(X_i)||,$$
 (1)

where X_i and x_i denote the 3D vertex on the input garment and its corresponding 2D position on the SMPL UV map, respectively. And N is the total number of garment vertices.

3.2. Body-SMPL Correspondence

The body-SMPL correspondence maps vertices from a 3D humanoid body to the SMPL model, as shown in Fig. 4. Unlike clothing-SMPL correspondence, body-SMPL correspondence faces challenges due to extreme proportions and

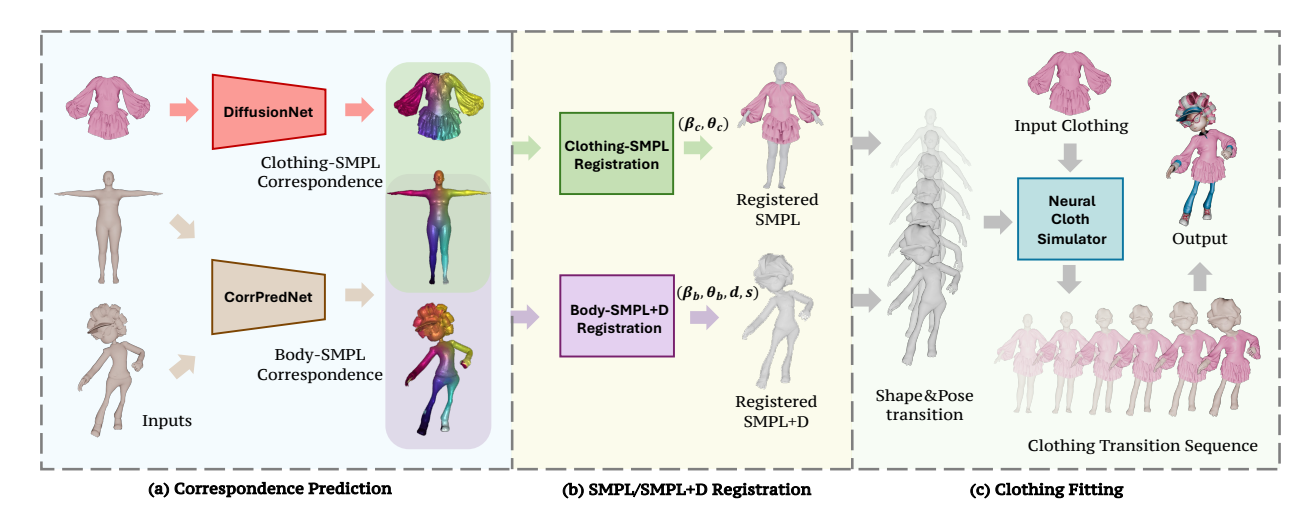


Figure 2. The overview of our LUIVITON system. (a) A modified DiffutionNet is used to compute the clothing-SMPL correspondence from the input clothing. Simultaneously, taking SMPL and the target character body as inputs, we predict the body-SMPL correspondence with our CorrPredNet. (b) Given the SMPL-based correspondences, we optimize the parameters of SMPL and SMPL+D by using two registration modules, which align SMPL to input clothing and body, respectively. (c) We perform interpolations between the registered SMPL and SMPL+D (with additional displacements and scale) to generate a smooth motion sequence with shape and pose transitions. Given this sequence and clothing as input, the neural cloth simulator produces a realistic and natural fit.

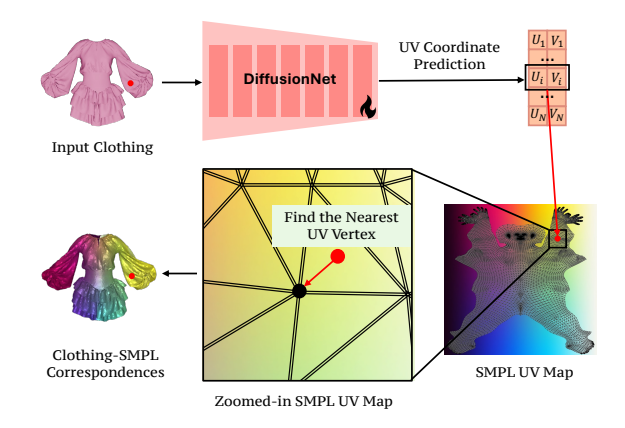


Figure 3. The clothing-SMPL correspondence module utilizes an adapted DiffusionNet to predict UV coordinates for clothing vertices, which are then used to establish correspondences between clothing and SMPL in UV space.

diverse poses, making geometric features less effective. Instead, semantic features offer a more robust solution.

We introduce the Correspondence Prediction Network (CorrPredNet), a diffusion model-based approach, which leverages semantic features extracted from 2D vision foundation models. Specifically, we input multi-view depth images into a synchronized diffusion model and DINOv2 [40] to obtain dense per-pixel semantic features. Following prior works [20, 53], these 2D features are unprojected into 3D using known camera parameters, yielding per-vertex feature embeddings for both the input body and the SMPL model. Correspondence is then established by computing

cosine similarity between the two sets of 3D features. To improve robustness, we introduce a noise filtering module that removes outlier correspondences before registration.

View-Consistent Feature Extraction. As shown in Fig. 4, we begin by rendering multi-view depth maps of the input 3D mesh, which are then passed to the SyncMVD [34] model to synthesize consistent and semantically plausible multi-view textures. During texture generation, we extract diffusion features from the last three layers of the UNet to capture rich and comprehensive semantic information across multiple feature scales. Specifically, for each view, the features are extracted during the denoising process for steps $t \geq 0.4T$, where T is the total number of denoising steps. To fuse diffusion features across different time steps, we upsample all the features to the same resolution and adopt a weighted fusion strategy defined as follows:

$$f_{\text{diff}}^{(n)} = \sum_{t=0.4T}^{T} f_{\text{diff},t}^{(n)} \cdot w_t, \quad n \in \{0, 1, 2\}$$
 (2)

$$w_t = \frac{t - 0.4T}{T - 0.4T} \cdot (1 - w_{\min}) + w_{\min},$$
 (3)

where $f_{\mathrm{diff},t}^{(n)}$ denotes the diffusion feature extracted at time step t from layer n, and w_t is the corresponding weight. The weighting function linearly increases from a minimum value w_{\min} at t=0.4T to 1.0 at t=T, which places more emphasis on features from the noisier stages while still retaining contributions from the cleaner ones. We empirically set $w_{\min}=0.1$ in our method.

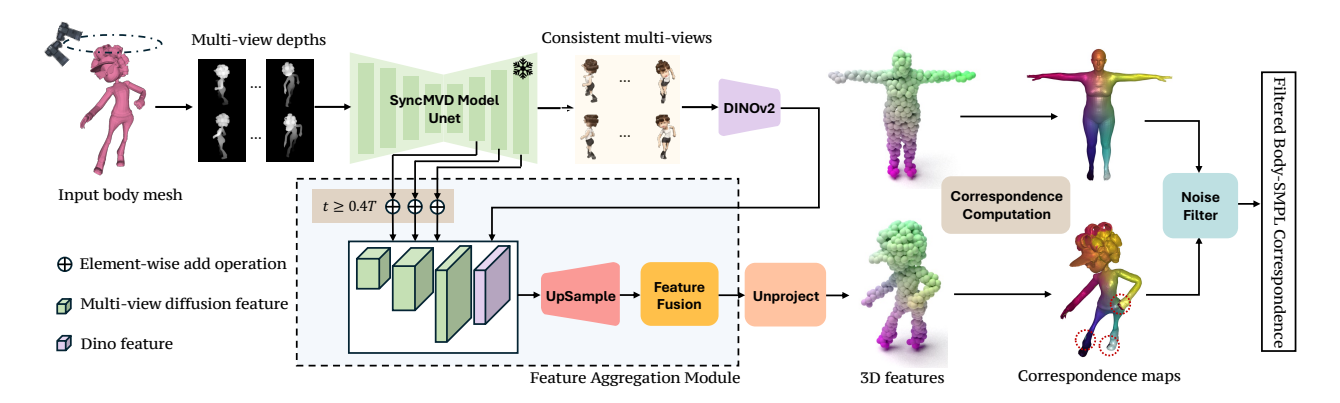


Figure 4. Starting from a humanoid body mesh, we first render multi-view depth maps and feed them into SyncMVD to generate consistent multi-view images. Next, we introduce a feature aggregation module that combines diffusion features from the SyncMVD U-Net with semantic features from DINOv2. These aggregated features are then unprojected onto the input meshes to form 3D features, which drive the computation of the correspondence. Finally, a noise filtering module is applied to identify the noise (highlighted by red circle) and produce clean Body-to-SMPL correspondences.

The consistent multi-view images generated by SyncMVD [34] are sent to DINOv2 [40] to extract semantic features. We propose a Feature Aggregation Module that produces the fused representation $f_{\rm fuse}$ to integrate diffusion and semantic features. Details of this module are provided in the Suppl. B.2.

Although the current stage successfully establishes initial correspondences, alignment errors, particularly in the limbs, persist due to the left-right ambiguity in the diffusion and semantic features. These errors can result in inaccurate correspondences and ultimately compromise the quality of SMPL registration. To address this issue, we introduce a noise filter module.

Noise Filter. We propose an energy-based iterative noise filter that removes unreliable correspondences based on local shape differences, thereby improving the robustness of subsequent registration.

For each input body vertex v_i , we define its K-ring neighborhood \mathcal{N}_i . For every neighbor vertex $v_j \in \mathcal{N}_i$, we compute the relative difference vectors p_j and q_j for every neighbor of vertex v_i as:

$$p_j = v_j - v_i$$
 and $q_j = \tilde{v}_j - \tilde{v}_i$, (4)

where v_i and v_j are vertices from the source mesh, v_j is a neighbor of v_i , and \tilde{v}_i and \tilde{v}_j are their corresponding vertices in SMPL. These vectors capture both distance and orientation differences while factoring out translations.

The optimal rotation matrix R_i is determined via Singular Value Decomposition (SVD) of the covariance matrix constructed from the p_j and q_j . The deformation energy for vertex i is defined as:

$$E_{i} = \sum_{j \in \mathcal{N}_{i}} \|q_{j} - R_{i} p_{j}\|^{2}.$$
 (5)

This energy measures local misalignment based on contributions from all K-ring neighbors. At each iteration, we compute E_i for all vertices. A dynamic threshold $\epsilon = \mu_E + 0.5\,\sigma_E$ is set to filter the vertices with higher energy, where μ_E and σ_E are the mean and standard deviation of the energies. And for each iteration, the neighborhood size is dynamically increased as $K = \text{iter}^2$, with iter representing the current iteration index, progressively incorporating a broader local context. This iterative process continues until the number of valid correspondences stabilizes or a maximum of four iterations is reached, ensuring robust noise filtering. By penalizing local misalignments, the filter helps resolve left-right ambiguities, thus enhancing SMPL registration accuracy.

3.3. Body/Clothing Registration

As shown in Fig. 2 (b), the goal of this stage is twofold: (1) fit a SMPL model into the input clothing, and (2) align a SMPL+D model with the target body. We formulate the registration as the following two optimization problems.

Clothing-SMPL Registration. We optimize the SMPL parameters (θ_c, β_c) to align the SMPL within the input garment. The registration is guided by the following weighted loss function:

$$\mathcal{L} = \lambda_{c2s} \mathcal{L}_{c2s} + \lambda_{shape} \mathcal{L}_{shape} + \lambda_{pose} \mathcal{L}_{pose} + \lambda_{lap} \mathcal{L}_{lap} + \lambda_{pene} \mathcal{L}_{pene},$$
 (6)

where λ terms control the weighting of each loss. Specifically, \mathcal{L}_{c2s} enforces alignment between clothing and SMPL vertices, while \mathcal{L}_{shape} and \mathcal{L}_{pose} regularize shape and pose to prevent extreme unrealistic deformations. \mathcal{L}_{lap} ensures smooth deformations by averaging vertex positions, and

 \mathcal{L}_{pene} penalizes body-clothing interpenetration. This step ensures an accurate SMPL fit to the clothing while maintaining realism and preventing penetration.

Body-SMPL+D Registration. We optimize the SMPL+D parameters $(\theta_b, \beta_b, d, s)$, where d allows fine per-vertex displacement, and $s \in \mathbb{R}^3$ controls scaling along the x,y,z axes. Scaling is essential for adapting SMPL to characters with extreme proportions when minor displacements are insufficient.

The optimization minimizes the following objective:

$$\mathcal{L} = \lambda_{b2s} \mathcal{L}_{b2s} + \lambda_{s2b} \mathcal{L}_{s2b} + \lambda_{corres} \mathcal{L}_{corres} + \lambda_{shape} \mathcal{L}_{shape} + \lambda_d \mathcal{L}_d + \lambda_s \mathcal{L}_s + \lambda_{lap} \mathcal{L}_{lap},$$
(7)

where \mathcal{L}_{b2s} and \mathcal{L}_{s2b} are the bidirectional point-to-mesh distances between the SMPL surface and the input body mesh, while \mathcal{L}_{corres} minimizes the distance between corresponding vertices with noise-filtered correspondence. \mathcal{L}_{s} regularizes scaling to avoid extreme unrealistic deformations, and \mathcal{L}_{d} constrains displacements for natural alignment. By jointly optimizing these terms, our method achieves robust and accurate SMPL+D registration across a wide range of body shapes and poses. All loss definitions used in clothing-SMPL and body-SMPL+D registration are detailed in Suppl. B.5.

3.4. Clothing Fitting and Resizing

In the Clothing Fitting stage (Fig. 2 (c)), body shape and pose are iteratively adjusted to transfer clothing from the source SMPL model onto the target SMPL+D model, dressing the input humanoid body.

Given the SMPL parameters (θ_c, β_c) and SMPL+D parameters $(\theta_b, \beta_b, d, s)$, we generate a motion sequence that smoothly transitions SMPL to SMPL+D via parametric interpolation. Since SMPL is a special case of SMPL+D, represented as $(\theta_c, \beta_c, d = \mathbf{0} \in \mathbb{R}^{6890 \times 3}, s = (1, 1, 1))$, interpolation allows for seamless adaptation of clothing.

Using this motion sequence, we fit clothing from the registered SMPL(θ_c , β_c) to the registered SMPL+D(θ_b , β_b , d, s) by ContourCraft[24], a state-of-the-art neural cloth simulator. ContourCraft ensures realistic dressing behavior while maintaining garment size under physical constraints. This enables flexible clothing size control through three modes:

- **Default Mode:** Retains the original clothing size for draping.
- **Auto-resized Mode:** Adjusts clothing size automatically for a better fit to the input body.
- **Customized Mode:** Enables clothing size customization by scaling the rest position of the garment geometry.

The auto-resize model utilizes body scale parameters from body-SMPL+D registration (Sec. 3.3) to adaptively

adjust the rest position of clothing with scale factors along the x, y, and z axes, ensuring seamless resizing across different body proportions. After the default mode, neither the auto-resized nor customized mode requires recomputing shape correspondences or registration. Once SMPL/SMPL+D is registered to the clothing and body, it can be reused across modes for efficient size adjustments.

4. Experiments

We evaluate each stage of our pipeline, compare with state-of-the-art methods, and conduct ablations to analyze key design choices. Dataset and implementation details are in Suppl. A and Suppl. B, while expert and user study results are in Suppl. E.5 and Suppl. G.

4.1. Qualitative Results

Fig. 5 demonstrates qualitative results of our system across default, auto-resized, and customized modes. It preserves garment shape in default mode, automatically adjusts fit in auto-resized mode, and supports user-defined scaling in customized mode. Our method handles diverse garment types and character shapes, including bulky, non-human, and stylized bodies, showcasing its robustness and broad applicability. Additional results are provided in Suppl. D.

4.2. Comparisons with Approaches on Clothing Draping

For comparative evaluation on overall clothing draping performance, we evaluate our method on the Cloth3D [6] test set against DrapeNet [17] and ISP [31], using 100 top-trouser pairs across 4 diverse poses each. Metrics include Chamfer Distance (CD), Point-to-Mesh (P2M), and Interpenetration Ratio (IR). Since the two methods can only take parametric bodies (SMPL) as input, for a fair comparison, we omit the *Body-SMPL correspondence prediction* and *Body-SMPL+D registration* stages from our pipeline and also use SMPL parameters as input.

Table 1. Comparison of clothing draping performance.

		Тор			Trousers		
$CD\downarrow$	P2M↓	IR(%)↓	CD↓	P2M↓	IR(%)↓		
0.0101	0.0100	1.58	0.0013	0.0012	4.12		
0.0034	0.0032	13.02	0.0081	0.0080	22.2		
0.0008	0.0007	0.56	0.0006	0.0005	0.20		
(0.0101	0.0101 0.0100 0.0034 0.0032	0.0101	0.0101 0.0100 1.58 0.0013 0.0034 0.0032 13.02 0.0081	0.0101 0.0100 1.58 0.0013 0.0012 0.0034 0.0032 13.02 0.0081 0.0080		

As shown in Tab. 1, our method achieves the lowest CD, P2M, and IR. Visual results in Fig. 6 further confirm that our predictions closely match the ground truth and exhibit the fewest artifacts among all methods. Additional results are provided in Suppl. E.1.



Figure 5. Our system can dress a wide range of garments on various humanoid bodies in diverse poses, with all three modes delivering plausible results.

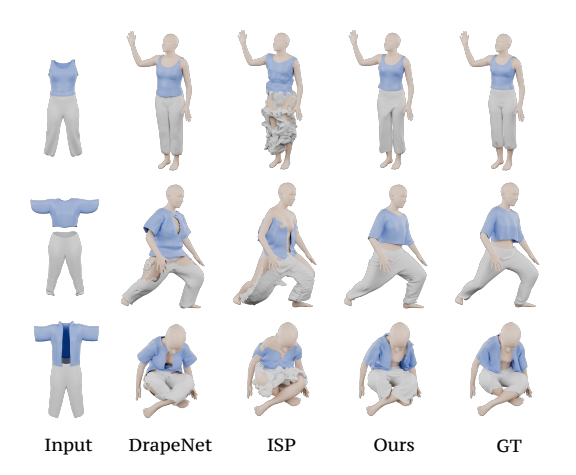


Figure 6. Qualitative comparisons with DrapeNet and ISP

4.3. Evaluation on Clothing-SMPL Correspondence and Registration

We evaluate our clothing-SMPL correspondence method on 100 garment-body pairs from the GarmentCode dataset [27], where each sample consists of a garment mesh and its paired SMPL body. Performance is evaluated using Mean Euclidean Error (MEE) and Mean Geodesic Error (MGE) between predicted and ground-truth correspondences, and Interpenetration Ratio (IR) after registration to quantify physical realism.

Table 2. Comparison of clothing-SMPL correspondence and registration performance.

Method	MGE ↓	MEE ↓	IR (%)↓	No-Penetration Rate ↑
CorrPredNet	0.2290	0.0993	1.02	5%
Ours	0.0499	0.0274	0.17	59%

We adopt the training-free CorrPredNet (originally developed for body correspondence) as a baseline since it provides an alternative possibility for unifying the framework. As shown in Tab. 2, our method significantly outperforms CorrPredNet. Our method yields zero interpenetration in 59% of cases, while CorrPredNet struggles with partial-to-complete mappings, resulting in inaccurate correspondences and unrealistic SMPL fits.

Qualitative results in Fig. 7 further illustrate this difference. For instance, in the fourth column, CorrPredNet incorrectly maps the lower hem of the dress to the feet, distorting the SMPL pose. Our method avoids such errors and produces clean, well-registered fits across diverse garment types.

4.4. Evaluation on Body-SMPL Correspondence and Registration

We introduce a new benchmark of eight stylized humanoid characters for a challenging evaluation, each with ten randomly sampled diverse poses. Details are provided in

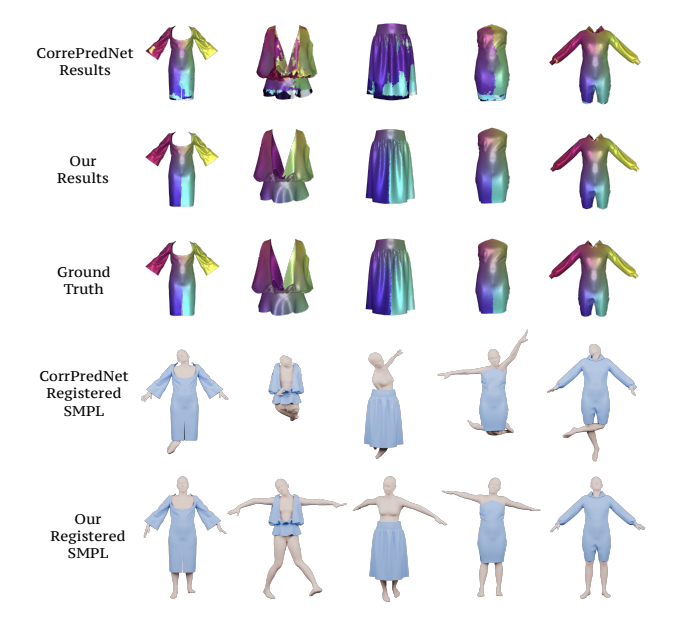


Figure 7. Qualitative comparison of clothing-SMPL correspondence. Compared to using CorrPredNet (top), our method (middle) yields more accurate correspondence results and SMPL registrations.

Suppl. A.2

Table 3. Comparison of body-SMPL correspondence performance across different methods.

Method	$\mathbf{MEE}(\times\ 10)\downarrow$	$\mathbf{MGE}(\times\ 10)\downarrow$
GeomFmaps	3.400	6.867
ULRSSM	3.224	6.442
Hybrid GeomFmaps	3.429	6.966
Hybrid ULRSSM	3.215	6.549
DiffusionNet	5.270	5.900
Diff3f	2.320	3.110
Ours	1.700	2.100

Body-SMPL Correspondence Evaluation. We evaluate our meth-od against GeomFmaps [19], ULRSSM [13], HybridFmaps [5], DiffusionNet [50], and Diff3f [20]. DiffusionNet is trained on 2,000 samples using our supervision strategy (Sec. 3.1), while others use public checkpoints. As shown in Tab. 3, our method achieves the lowest average MEE and MGE. Furthermore, functional map methods struggle with unseen topologies; DiffusionNet lacks robustness to shape and pose, and Diff3f improves with semantic priors. Our method further improves coherence and consistency(see Fig. 8).

Evaluation of Body-SMPL Registration We evaluate SMPL registration accuracy against NICP [38] and

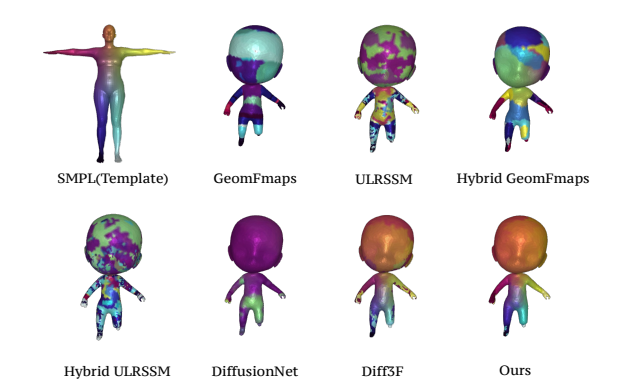


Figure 8. Qualitative comparison of GeomFmaps, ULRSSM, Hybrid GeomFmaps (Hybrid GFM), Hybrid ULRSSM, Diffusion-Net, Diff3f, and our method predicting body correspondence.

Diff3f [20] using Chamfer Distance between the registered SMPL+D and input body mesh. As shown in Tab. 4, our approach achieves the lowest CD, indicating superior registration quality. Furthermore, the proposed noise filtering module plays a critical role in enhancing alignment accuracy. Visual comparisons in Fig. 9 show that NICP fails to generalize to the character with extreme body shapes (big head and small body), while Diff3f exhibits limitations under large pose deformations. In contrast, our method demonstrates consistently robust and precise registrations across diverse test cases. Notably, even without noise filtering, our method outperforms all baselines, and the integration of the filter further boosts performance. More discussions can be found in Suppl. E.3.



Figure 9. Qualitative comparisons of the performance of Body-SMPL+D registration.

Table 4. Comparison of Chamfer Distance for body-SMPL registration.

Method	NICP	Diff3f (w/o Filter)	Diff3f (w/ Filter)	Ours (w/o Filter)	Ours (w/ Filter)
CD ×10 ⁻⁴ ↓	13.05	4.99	4.49	1.46	1.19

4.5. Ablation Study

Ablation Study on Viewpoint Choices for Body-SMPL Correspondence We analyze the impact of viewpoint selection by varying azimuthal density and camera elevation in the depth-image-based correspondence prediction pipeline (Fig. 4). The camera elevation angles of 30°/15°

yield optimal performance, achieving 0.94% to 14.98% lower MGE compared to other settings. For azimuthal coverage, we find that 18 views per elevation level (totaling 36 views) provides the most accurate correspondences, outperforming other configurations by 2.33% to 7.89% in terms of MGE reduction. Complete quantitative results and qualitative comparisons are presented in Suppl. F.1 and Suppl. F.2, respectively.

Ablation Study on Feature Aggregation Strategies for Body-SMPL Correspondence We evaluate different combinations of diffusion and DINOv2 features for correspondence prediction. The best performance is achieved by aggregating multi-scale features from multiple diffusion layers and combining them with DINOv2 features, resulting in 2.33% to 62.03% lower MGE compared to other strategies. Detailed results are provided in Suppl. F.3.

Ablation Study on Body-SMPL+D Registration Accurate body-SMPL registration is crucial since the clothing is finally fitted on the registered SMPL. We ablate key components of our body registration pipeline: the noise filter, pervertex displacements (*d*), and the learnable scale parameter (*s*).

Table 5. Ablation study on Body-SMPL+D registration components.

Method	Ours	Ours (w/o Filter)	Ours (w/o d)	Ours (w/o Filter, d)	Ours (w/o Filter, d, s)
CD (×10 ⁻⁴) ↓	1.19	1.46	9.55	9.22	9.63

As shown in Tab. 5, removing the noise filter increases CD, while excluding d leads to a significant performance drop, confirming its importance for adapting SMPL to diverse and complex body shapes. Disabling both retains high error, indicating their complementarity. Fig. 10 further shows that these components are critical for accurate registration and clean clothing fitting. More results are in Suppl. F.4.

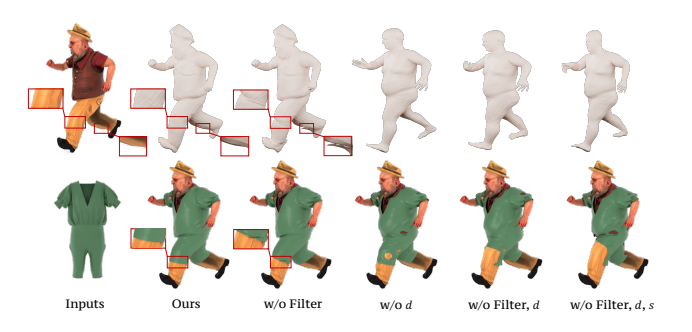


Figure 10. Ablation of body registration.

Ablation Study on Correspondence Modules. We assess the impact of correspondence quality on final garment fitting by replacing our body-to-SMPL and clothing-to-SMPL modules with next-best alternatives, Diff3f and CorrPredNet, respectively. While quantitative comparisons are reported in Sec. 4.4 and Sec. 4.3, this ablation focuses on the effect of each correspondence module on the final visual outcome. The study is conducted on 5 stylized characters with varied garments and is evaluated via a user study (Suppl. G.5).

As shown in Fig. 11, inaccurate body correspondence (b) leads to incorrect SMPL shape and poor clothing deformation, while inaccurate clothing correspondence (c) causes severe interpenetration, such as limbs poking through the garment. When both are suboptimal (d), the errors compound, resulting in the worst overall fitting. In contrast, our full method (a) achieves realistic draping. Additional results are provided in Suppl. F.5.

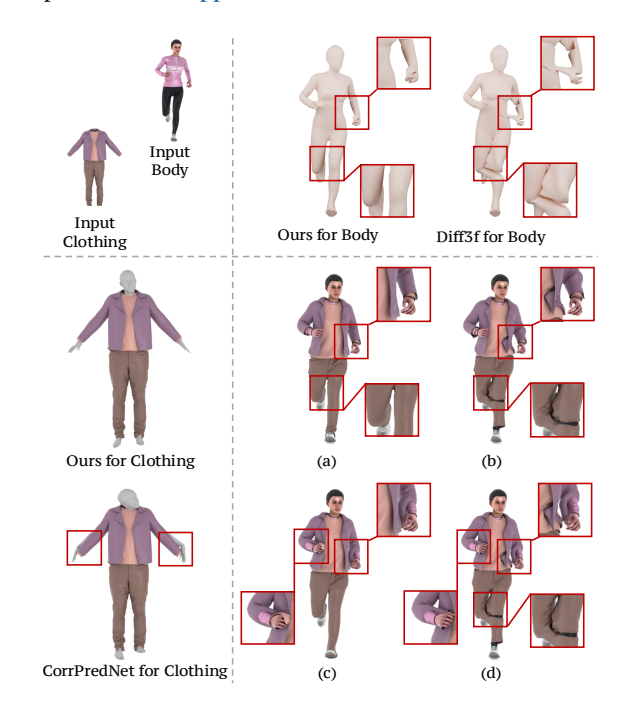


Figure 11. Ablation on Correspondence Module

4.6. Material Behavior

Our system supports customizable material parameters to simulate different fabric types. As shown in Fig. 12, increasing stiffness yields less deformation and better shape retention. This enables flexible control over garment behavior for various virtual try-on scenarios.

4.7. Applications

Our system enables clothing to be draped onto posed characters, making it ideal for animation initialization. As

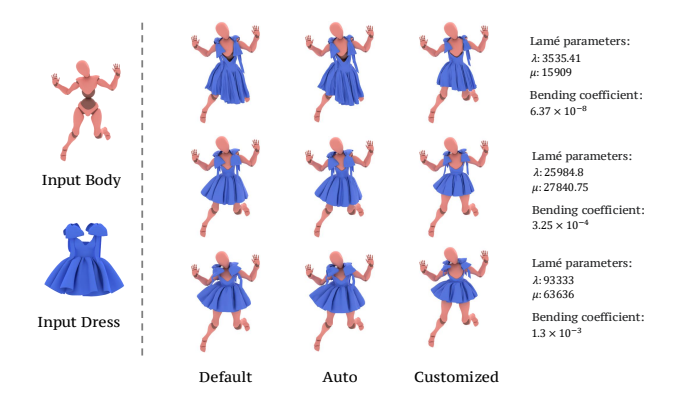


Figure 12. Effect of material parameters on a dress. As Lamé parameters (λ,μ) and the bending coefficient increase from top to bottom, the dress becomes stiffer, retaining more of its shape.

shown in Fig. 13, clothing is fitted to the first frame and then simulated using Marvelous Designer [22]. It also supports large-scale generation of synthetic clothed human scans (Fig. 5). With a small number of tight-clothed scans, we can synthesize diverse clothed identities for tasks such as 3D reconstruction, pose estimation, and virtual try-on. More discussions are in Suppl. H.



Figure 13. Our LUIVITON system can be applied to downstream tasks like dressing up a character for animation.

4.8. Limitations

Our system struggles with highly non-humanoid shapes (e.g., airplane in Fig. 14) where meaningful correspondences are failed to be established. It also has difficulty handling hard materials and disconnected clothing parts due to limitations in the simulator and physical constraints (Fig. 15). Additionally, clothing is currently limited to restpose input only. Further discussions are in Suppl. I.

5. Conclusion

In this paper, we presented LUIVITON, a fully automated virtual try-on framework capable of handling complex multilayer garments and fitting them to a wide range of models, including realistic humans, cartoon characters, and robots. Unlike traditional methods that either rely on manual intervention or are limited to parametric models and simple clothing, our automatic system generalizes to diverse body

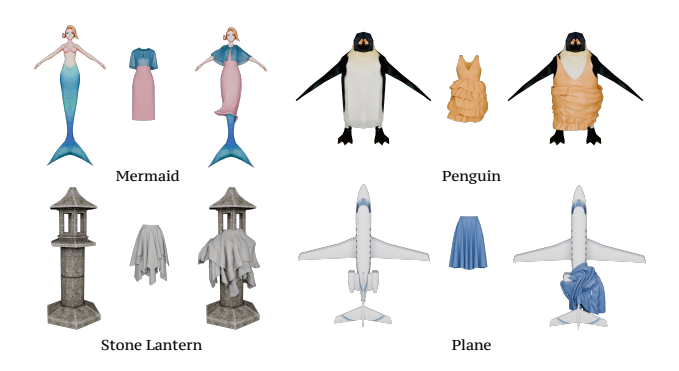


Figure 14. Applying our LUIVITON system to dress less humanoid models.

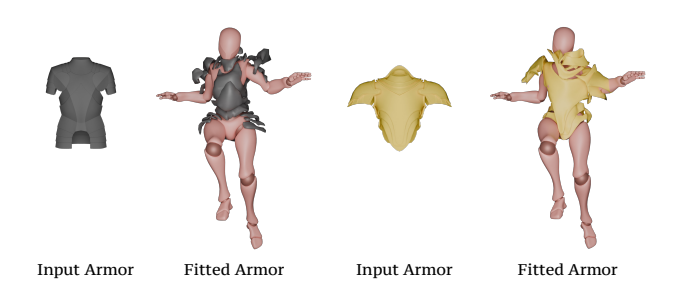


Figure 15. Our system fails to accurately fit hard and segmented material armors to the input body.

shapes and styles by leveraging SMPL as a proxy representation.

In particular, we have shown that we can effectively split clothing-to-body fitting into two correspondence tasks-clothing-SMPL (part-ial-to-complete alignment) and body-SMPL (large shape/pose variation). We have identified unique challenges to both correspondence problems. For the SMPL-clothing correspondence, we are focusing on a partial-to-complete alignment task, while for the SMPL-body correspondence, the shape/pose variations are particularly challenging. While a diffusion model-based approach for appearance correspondence is highly effective for body-to-SMPL fitting, pre-trained foundation models fail at handling the complexity of clothing deformations and textures. A geometric learning-based correspondence prediction approach based on DiffusionNet, however, is effective for computing dense partial-to-complete correspondences between complex clothing models in near-rest pose and an SMPL model.

We have further demonstrated key virtual try-on features using our LUIVITON framework for customizable garment sizing and material, making it practical for applications such as virtual try-on, gaming, and AR. We validated the robustness and versatility of our method across a wide range of body shapes, garment types, and poses, showing strong generalization to unseen clothing and characters without re-

training.

Future Work Our current approach uses an intermediate SMPL representation for mapping clothing to bodies. Since our method is highly robust, we hope to explore the ability to build a massive dataset with highly diverse clothed subjects and train a model that can directly map from any clothing to arbitrary characters. Furthermore, we believe that our technique, combined with a large database, is a key building block for generative apparel digitization, design, and editing.

References

- [1] Ahmed Abdelreheem, Abdelrahman Eldesokey, Maks Ovsjanikov, and Peter Wonka. Zero-shot 3d shape correspondence. In *SIGGRAPH Asia 2023 Conference Papers*, pages 1–11, 2023. 2
- [2] Yonathan Aflalo, Anastasia Dubrovina, and Ron Kimmel. Spectral generalized multi-dimensional scaling. *International Journal of Computer Vision*, 118:380–392, 2016.
- [3] Abderrazzak Ait Mouhou, Abderrahim Saaidi, Majid Ben Yakhlef, and Khalid Abbad. 3d garment positioning using hermite radial basis functions. *Virtual Reality*, pages 1–28, 2022. 3
- [4] Autodesk. Autodesk maya, 2025. 2
- [5] Lennart Bastian, Yizheng Xie, Nassir Navab, and Zorah Lähner. Hybrid functional maps for crease-aware nonisometric shape matching. In *Proceedings of the IEEE/CVF* Conference on Computer Vision and Pattern Recognition, pages 3313–3323, 2024. 8
- [6] Hugo Bertiche, Meysam Madadi, and Sergio Escalera. Cloth3d: clothed 3d humans. In European Conference on Computer Vision, pages 344–359. Springer, 2020. 6
- [7] Hugo Bertiche, Meysam Madadi, and Sergio Escalera. Pbns: physically based neural simulator for unsupervised garment pose space deformation. arXiv preprint arXiv:2012.11310, 2020. 3
- [8] Hugo Bertiche, Meysam Madadi, Emilio Tylson, and Sergio Escalera. Deepsd: Automatic deep skinning and pose space deformation for 3d garment animation. In *Proceedings* of the IEEE/CVF International Conference on Computer Vision, pages 5471–5480, 2021.
- [9] Hugo Bertiche, Meysam Madadi, and Sergio Escalera. Neural cloth simulation. *ACM Transactions on Graphics (TOG)*, 41(6):1–14, 2022. 3
- [10] Paul J Besl and Neil D McKay. Method for registration of 3-d shapes. In Sensor fusion IV: control paradigms and data structures, pages 586–606, 1992. 2
- [11] Bharat Lal Bhatnagar, Cristian Sminchisescu, Christian Theobalt, and Gerard Pons-Moll. Combining implicit function learning and parametric models for 3d human reconstruction. In *European Conference on Computer Vision*, pages 311–329. Springer, 2020. 2
- [12] Davide Boscaini, Jonathan Masci, Emanuele Rodolà, and Michael Bronstein. Learning shape correspondence with

- anisotropic convolutional neural networks. Advances in Neural Information Processing Systems, 29, 2016. 2
- [13] Dongliang Cao, Paul Roetzer, and Florian Bernard. Unsupervised learning of robust spectral shape matching. arXiv preprint arXiv:2304.14419, 2023. 8
- [14] Will Chang, Hao Li, Niloy J. Mitra, Mark Pauly, and Michael Wand. Geometric registration for deformable shapes. In Eurographics 2010: Tutorial Notes, 2010. 2
- [15] Will Chang, Hao Li, Niloy J. Mitra, Mark Pauly, Szymon Rusinkiewicz, and Michael Wand. Computing correspondences in geometric data sets. In *Eurographics 2011: Tuto*rial Notes, 2011.
- [16] Will Chang, Hao Li, Niloy J. Mitra, Mark Pauly, and Michael Wand. Dynamic geometry processing. In *Eurographics* 2012: Tutorial Notes, 2012.
- [17] Luca De Luigi, Ren Li, Benoît Guillard, Mathieu Salzmann, and Pascal Fua. Drapenet: Garment generation and self-supervised draping. In *Proceedings of the IEEE/CVF Conference on Computer Vision and Pattern Recognition*, pages 1451–1460, 2023. 2, 3, 6
- [18] Nicolas Donati, Abhishek Sharma, and Maks Ovsjanikov. Deep geometric functional maps: Robust feature learning for shape correspondence. In *Proceedings of the IEEE/CVF Conference on Computer Vision and Pattern Recognition*, pages 8592–8601, 2020. 2
- [19] Nicolas Donati, Abhishek Sharma, and Maks Ovsjanikov. Deep geometric maps: Robust feature learning for shape correspondence. CVPR, 2020. 8
- [20] Niladri Shekhar Dutt, Sanjeev Muralikrishnan, and Niloy J Mitra. Diffusion 3d features (diff3f): Decorating untextured shapes with distilled semantic features. In *Proceedings of* the IEEE/CVF Conference on Computer Vision and Pattern Recognition, pages 4494–4504, 2024. 2, 3, 4, 8
- [21] Danielle Ezuz and Mirela Ben-Chen. Deblurring and denoising of maps between shapes. In *Computer Graphics Forum*, pages 165–174. Wiley Online Library, 2017. 2
- [22] CLO Virtual Fashion. Marvelous designer: 3d clothing design software, 2025. Accessed: 2025-01-12. 2, 3, 10
- [23] Artur Grigorev, Michael J Black, and Otmar Hilliges. Hood: Hierarchical graphs for generalized modelling of clothing dynamics. In *Proceedings of the IEEE/CVF Conference* on Computer Vision and Pattern Recognition, pages 16965– 16974, 2023. 3
- [24] Artur Grigorev, Giorgio Becherini, Michael Black, Ot-mar Hilliges, and Bernhard Thomaszewski. ContourCraft: Learning to resolve intersections in neural multi-garment simulations. In ACM SIGGRAPH 2024 Conference Papers, pages 1–10, 2024. 3, 6
- [25] Luchen Huang and Ruoyu Yang. Automatic alignment for virtual fitting using 3d garment stretching and human body relocation. *The Visual Computer*, 32:705–715, 2016. 3
- [26] Varun Jain and Hao Zhang. Robust 3d shape correspondence in the spectral domain. In *IEEE International Conference* on Shape Modeling and Applications, pages 19–19. IEEE, 2006. 2
- [27] Maria Korosteleva, Timur Levent Kesdogan, Fabian Kemper, Stephan Wenninger, Jasmin Koller, Yuhan Zhang, Mario

- Botsch, and Olga Sorkine-Hornung. GarmentCodeData: A dataset of 3D made-to-measure garments with sewing patterns. In *European Conference on Computer Vision*, 2024.
- [28] Hao Li, Robert W Sumner, and Mark Pauly. Global correspondence optimization for non-rigid registration of depth scans. In *Computer Graphics Forum*, pages 1421–1430, 2008.
- [29] Hao Li, Bart Adams, Leonidas J Guibas, and Mark Pauly. Robust single-view geometry and motion reconstruction. ACM Transactions on Graphics (ToG), 28(5):1–10, 2009.
- [30] Jituo Li, Juntao Ye, Yangsheng Wang, Li Bai, and Guodong Lu. Fitting 3d garment models onto individual human models. *Computers & graphics*, 34(6):742–755, 2010. 3
- [31] Ren Li, Benoît Guillard, and Pascal Fua. Isp: Multi-layered garment draping with implicit sewing patterns. *Advances in Neural Information Processing Systems*, 36, 2024. 2, 3, 6
- [32] Zhong Li, Xiaogang Jin, Brian Barsky, and Jun Liu. 3d clothing fitting based on the geometric feature matching. In IEEE International Conference on Computer-Aided Design and Computer Graphics, pages 74–80, 2009. 3
- [33] Or Litany, Tal Remez, Emanuele Rodola, Alex Bronstein, and Michael Bronstein. Deep functional maps: Structured prediction for dense shape correspondence. In *Proceedings* of the IEEE/CVF International Conference on Computer Vision, pages 5659–5667, 2017. 2
- [34] Yuxin Liu, Minshan Xie, Hanyuan Liu, and Tien-Tsin Wong. Text-guided texturing by synchronized multi-view diffusion. In SIGGRAPH Asia 2024 Conference Papers, pages 1–11, 2024. 4, 5
- [35] Matthew Loper, Naureen Mahmood, Javier Romero, Gerard Pons-Moll, and Michael J Black. Smpl: A skinned multiperson linear model. In Seminal Graphics Papers: Pushing the Boundaries, pages 851–866. 2023. 2
- [36] Qianli Ma, Jinlong Yang, Anurag Ranjan, Sergi Pujades, Gerard Pons-Moll, Siyu Tang, and Michael J Black. Learning to dress 3d people in generative clothing. In *Proceedings* of the IEEE/CVF Conference on Computer Vision and Pattern Recognition, pages 6469–6478, 2020. 3
- [37] Robin Magnet and Maks Ovsjanikov. Memory-scalable and simplified functional map learning. In *Proceedings of the IEEE/CVF Conference on Computer Vision and Pattern Recognition*, pages 4041–4050, 2024. 2
- [38] Riccardo Marin, Enric Corona, and Gerard Pons-Moll. Nicp: neural icp for 3d human registration at scale. In *European Conference on Computer Vision*, pages 265–285. Springer, 2025. 2, 8
- [39] Rahul Narain, Armin Samii, and James F O'brien. Adaptive anisotropic remeshing for cloth simulation. *ACM transactions on graphics (TOG)*, 31(6):1–10, 2012. 3
- [40] Maxime Oquab, Timothée Darcet, Théo Moutakanni, Huy Vo, Marc Szafraniec, Vasil Khalidov, Pierre Fernandez, Daniel Haziza, Francisco Massa, Alaaeldin El-Nouby, et al. Dinov2: Learning robust visual features without supervision. arXiv preprint arXiv:2304.07193, 2023. 2, 3, 4, 5
- [41] Maks Ovsjanikov, Mirela Ben-Chen, Justin Solomon, Adrian Butscher, and Leonidas Guibas. Functional maps: a flexible

- representation of maps between shapes. ACM Transactions on Graphics (TOG), 31(4):1–11, 2012. 2
- [42] Xiaoyu Pan, Jiaming Mai, Xinwei Jiang, Dongxue Tang, Jingxiang Li, Tianjia Shao, Kun Zhou, Xiaogang Jin, and Dinesh Manocha. Predicting loose-fitting garment deformations using bone-driven motion networks. In ACM SIG-GRAPH 2022 Conference Papers, pages 1–10, 2022. 3
- [43] Chaitanya Patel, Zhouyingcheng Liao, and Gerard Pons-Moll. Tailornet: Predicting clothing in 3d as a function of human pose, shape and garment style. In *Proceedings of* the IEEE/CVF Conference on Computer Vision and Pattern Recognition, pages 7365–7375, 2020. 2, 3
- [44] Gerard Pons-Moll, Sergi Pujades, Sonny Hu, and Michael J Black. Clothcap: Seamless 4d clothing capture and retargeting. ACM Transactions on Graphics (TOG), 36(4):1–15, 2017. 3
- [45] Emanuele Rodolà, Luca Cosmo, Michael M Bronstein, Andrea Torsello, and Daniel Cremers. Partial functional correspondence. In *Computer Graphics Forum*, pages 222–236. Wiley Online Library, 2017. 2
- [46] Robin Rombach, Andreas Blattmann, Dominik Lorenz, Patrick Esser, and Björn Ommer. High-resolution image synthesis with latent diffusion models. In *Proceedings of* the IEEE/CVF Conference on Computer Vision and Pattern Recognition, pages 10684–10695, 2022. 3
- [47] Igor Santesteban, Miguel A Otaduy, and Dan Casas. Learning-based animation of clothing for virtual try-on. In Computer Graphics Forum, pages 355–366. Wiley Online Library, 2019. 3
- [48] Igor Santesteban, Nils Thuerey, Miguel A Otaduy, and Dan Casas. Self-supervised collision handling via generative 3d garment models for virtual try-on. In *Proceedings of the IEEE/CVF Conference on Computer Vision and Pattern Recognition*, pages 11763–11773, 2021.
- [49] Igor Santesteban, Miguel A Otaduy, and Dan Casas. Snug: Self-supervised neural dynamic garments. In Proceedings of the IEEE/CVF Conference on Computer Vision and Pattern Recognition, pages 8140–8150, 2022. 3
- [50] Nicholas Sharp, Souhaib Attaiki, Keenan Crane, and Maks Ovsjanikov. Diffusionnet: Discretization agnostic learning on surfaces. ACM Transactions on Graphics (TOG), 41(3): 1–16, 2022. 3, 8
- [51] Guangyuan Shi, Chengying Gao, Dong Wang, and Zhuo Su. Automatic 3d virtual fitting system based on skeleton driving. *The Visual Computer*, 37:1075–1088, 2021. 3
- [52] Lokender Tiwari and Brojeshwar Bhowmick. Deepdraper: Fast and accurate 3d garment draping over a 3d human body. In *Proceedings of the IEEE/CVF International Conference on Computer Vision*, pages 1416–1426, 2021. 2
- [53] Lingyu Wei, Qixing Huang, Duygu Ceylan, Etienne Vouga, and Hao Li. Dense human body correspondences using convolutional networks. In *Proceedings of the IEEE conference* on computer vision and pattern recognition, pages 1544– 1553, 2016. 2, 4
- [54] Nannan Wu, Zhigang Deng, Yue Huang, Chen Liu, Dongliang Zhang, and Xiaogang Jin. A fast garment fitting algorithm using skeleton-based error metric. *Computer Animation and Virtual Worlds*, 29(3-4):e1811, 2018. 3

- [55] Wang Zeng, Wanli Ouyang, Ping Luo, Wentao Liu, and Xiaogang Wang. 3d human mesh regression with dense correspondence. In *Proceedings of the IEEE/CVF Conference on Computer Vision and Pattern Recognition*, pages 7054–7063, 2020. 3
- [56] Silvia Zuffi and Michael J Black. The stitched puppet: A graphical model of 3d human shape and pose. In *Proceedings of the IEEE Conference on Computer Vision and Pattern Recognition*, pages 3537–3546, 2015. 2